CrystEngComm

Accepted Manuscript

ROYAL SOCIETY OF CHEMISTRY

www.rsc.org/crystengcomm

Journal Name

ARTICLE

A Study on the Influence of Sodium Carbonate Concentration on the Synthesis of High Mg Calcite

Received 00th January 20xx,
Accepted 00th January 20xx

DOI: 10.1039/x0xx00000x

www.rsc.org/

Heng Yang, Shiqiang Chai, Yuzhe Zhang, Yurong Ma*

Well crystallized high Mg calcites in pure phase with Mg contents higher than 50 mol%, so called proto-dolomite, has not been synthesized in the laboratories to our knowledgement. In this work, the synthesis of high Mg calcites in pure phase with Mg contents controlled from 10 to 63 mol% was realized by using amorphous calcium magnesium carbonate as intermediate precursor phase through a hydrothermal process in the absence of any organic additive. Besides the molar ratios of $[Mg^{2+}]/[Ca^{2+}]$, the molar ratios of carbonate and calcium ion in the mother solutions are also very important for the Mg contents in the high Mg calcites in pure phase. The higher molar ratios of $[CO_3^{2-}]/[Ca^{2+}]$ in the mother solutions, the higher Mg contents in Mg calcites in pure phase can be obtained at relatively low carbonate concentrations. It is the first time to report for the variation of Mg contents in the high Mg calcites by changing the molar ratios of $[CO_3^{2-}]/[Ca^{2+}]$ in the mother solutions in this work. Further increase of carbonate concentration results in the formation of other crystal phases such as Ca-magnesite, brucite, or aragonite. Studies on the structural analysis and formation mechanisms of thermodynamically unstable biogenic high-Mg calcite minerals may shed light on the preparation of functional materials with enhanced mechanical properties.

Introduction

High magnesium-bearing calcite crystals with Mg contents higher than 10 mol% are a thermodynamically unstable phase of calcium carbonate under ambient conditions,[1-3] which are normally synthesized under high temperature and high pressure in the laboratories.[4-6] However, biogenic calcites with very high Mg contents (20-43 mol%) has been found in many marine organisms such as coralline algae,[7] Alcyonarian corals,[8] echinoids sea urchins[9, 10] and sea stars.[11] How marine organisms form high Mg calcite under ambient conditions has been an enigma for a long time. Amorphous calcium magnesium carbonate (ACMC) was supposed to be an intermediate precursor phase for the formation of biogenic high Mg calcites in biominerals.[12-15] It was reported that magnesium plays a key role for stabilizing the amorphous calcium carbonate (ACC) phase[2, 16, 17] and for improving the mechanical properties of biogenic Mg calcites.[18, 19] Therefore, studying the formation mechanism of high Mg calcites not only has great importance in fundamental research of biomineralization but may also shed light on the design and fabrication of new functional materials.

The synthesis of Mg-bearing calcites has been succeeded under ambient conditions in the last years with the help of intermediate amorphous phase,[2, 20, 21] mixed solvents,[22-25] organic/inorganic surfaces,[26] and soluble additives.[20, 25, 27-32] Mg content in the high Mg calcites was considered to be positively related to the $[Mg^{2+}]/[Ca^{2+}]$ molar ratio in the reaction solution.[20, 30, 33] Raz et al. synthesized magnesium calcite particles with 34 mol% of magnesium along with aragonite in the presence of macromolecules extracted from skeletons of coralline algae.[2] Calcite with at most 15 mol% magnesium content and aragonite were produced by using additives that contain alcohols[22] or carboxylate groups[27, 30, 34] that usually occur in biomineral organisms in solutions. Cheng et al. produced high magnesium-bearing calcite films via polymer induced liquid precursor process which contain up to 26 mol% magnesium but with low crystallization degree.[29] Compared with biogenic high magnesium-bearing calcites, these synthesized Mg-bearing calcite products often contain considerable amount of aragonite,[2, 21, 22, 25, 27] as well as a certain amount of ACC.[29] The synthesis of thermodynamically unstable high Mg calcite in pure phase is especially difficult under ambient conditions. It is hard for Mg^{2+} to be inserted into the calcite lattices because of the bigger hydration radii of Mg^{2+} ion than that of Ca^{2+} ion[35], which is attributed to the higher solvation free energy[36] and the higher dehydration enthalpy[34] of Mg^{2+} ion than that of Ca^{2+} ion at room temperature. There is a fundamental barrier that prevents the formation of long range ordered structures of Mg^{2+} and CO_3^{2-} resulted by the lattice limitation on the spatial structure of carbonate group in high Mg carbonate minerals (i.e., dolomite and magnesite).[37] Our group succeeded the synthesis of high Mg calcites in pure phase with Mg content as high as 43 mol% via polymer stabilized ACMC precursors under ambient conditions.[20]

College of Chemistry, Peking University, Beijing,100871, China. Fax: 086-1062751708; Tel: 086-1062753269; E-mail: yurong.ma@pku.edu.cn

† Footnotes relating to the title and/or authors should appear here.

Electronic Supplementary Information (ESI) available: [details of any supplementary information available should be included here]. See DOI: 10.1039/x0xx00000x

Aqueous carbonate accumulation and the pH value of the sea water are important for the mineralization rates of biogenic calcium carbonate in the marine organisms. It was pointed out that the calcification rates for marine organisms decline along with the carbonate concentration owing to its reaction with increasing concentration of anthropogenic CO_2.[38] Furthermore, it was found that aqueous carbonate concentration influences the polymorphs of calcium carbonate while the $[CO_3^{2-}]/[Ca^{2+}]$ molar ratio is in between $10^{-1.5}$ ~$10^{-3.5}$.[39] However, the influence of the $[CO_3^{2-}]/[Ca^{2+}]$ ratio on the crystallization process of magnesium containing calcium carbonate has not been investigated as far as we know. The effect of relatively high $[CO_3^{2-}]/[Ca^{2+}]$ molar ratio (>0.1) or relative high carbonate concentration (> 0.05 mol/L) on the polymorph of calcium carbonate has not been studied up to now.

The aim for this work is to study the influence of the molar ratios of $[CO_3^{2-}]/[Ca^{2+}]$ and $[Mg^{2+}]/[Ca^{2+}]$ on the crystal phases of carbonate minerals and the Mg contents in the Mg containing calcites. A hydrothermal process was applied for the synthesis of very high Mg calcites in pure phase by using ACMC as intermediate precursor.

Results and discussion

The amorphous precursor phase

White precipitates were quickly formed after mixing the metal chloride solution and sodium carbonate solution. These white precipitates were separated from the mother solution by filtration and dried for further characterizations. Scanning electron microscopy (SEM) and Transmission electron microscopy (TEM) images indicate that the white precipitates are composed of nanoparticles with size in the range of 25-60 nm (Figure 1 a and b). Selected area electron diffraction (SAED) pattern in figure 1b shows that the nanoparticles are in the amorphous phase, which is further confirmed by X-ray diffraction (XRD) pattern in Figure 1 c. Keeping in mind that calcium ion, magnesium ion and carbonate were present in the aqueous solutions, we assume that the white precipitates are composed of ACMC phase. The aqueous suspensions including the white nanoparticles were further treated with a hydrothermal process.

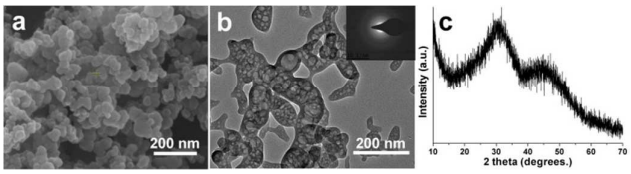

Figure 1. Characterizations on the intermediate amorphous phase of calcium (magnesium) carbonate at the early stage. (a) SEM image, (b) TEM image, (c) XRD pattern. The molar ratio for $[Mg^{2+}]$ and $[Ca^{2+}]$ in the mother solution was 2.

XRD characterizations

In a typical synthesis, the freshly prepared cloudy suspensions with different molar ratios of $[CO_3^{2-}]/[Ca^{2+}]$ were kept at 150 °C for 24 hours. The precipitates were separated from the mother solutions by filtration, washed with double distilled water and ethanol, and then dried at 70 °C for 24 hours. The final products were characterized in details by using XRD, SEM and Fourier transform infrared (FTIR) spectroscopy. The XRD patterns for the final products indicate that the primary phase for the products is Mg-containing calcite while changing the molar ratios of $[CO_3^{2-}]/[Ca^{2+}]$ in the mother solution from 0.56 to 6.11 at an $[Mg^{2+}]/[Ca^{2+}]$ ratio of 2 (Figure 2). With the increase of $[CO_3^{2-}]/[Ca^{2+}]$ ratios from 0.28 to 2.78, the final products are in the pure phase of Mg-containing calcite and the diffraction peaks shift to higher 2 theta (figure 2), which is more clearly from the $(10\bar{1}4)$ peak movement at 2 theta in the range of 29 ~ 33 ° scanned with a slow rate (0.2 °/min). Lattice spacings of Mg containing calcites decrease when Mg^{2+} ion replaces the position of Ca^{2+} ion in the lattice of calcite crystal because the radius of Mg^{2+} is smaller than that of Ca^{2+}.[4] Thus the diffraction peaks of Mg containing calcite shift to higher 2 theta values and the Mg contents in the Mg-calcites can be calculated by using the shifts of the 2 theta values of $(10\bar{1}4)$ peak according to the formula (1) in the literature[4]:

$$\text{Mg mol.}-\% = \frac{2\theta_{\text{Mg-Calcite}} - 2\theta_{\text{Calcite}}}{2\theta_{\text{Magesite}} - 2\theta_{\text{Calcite}}} \qquad (1)$$

The Mg content is given as a molar percentage relative to the number of Ca^{2+} ions in the calcite lattice such that the sum of Ca mol% and Mg mol% in the samples is 100%. The Mg contents of the obtained Mg-calcite products in pure phase increase from 8.7 mol% to 58 mol% while increasing the molar ratios of $[CO_3^{2-}]/[Ca^{2+}]$ from 0.56 to 2.78 according to the above mentioned formula. High Mg calcite mesocrystals with Mg contents as high as 53 mol% mixed with aragonite was synthesized in an organic solvent/water mixture by Lenders and collaborators.[25] However, this is the first time to obtain well crystallized pure phase high Mg calcites with Mg contents higher than 50 mol%, as far as we know. More importantly, no organic additives was applied to tune the polymorphs in the reaction solutions during the synthesis of pure phase high Mg-calcites. Recently, our group reported the synthesis of high Mg calcites with controlled magnesium content from 15 to 40 mol% via polymer stabilized amorphous precursors under ambient conditions.[20]

Besides Mg-calcite as the primary crystalline phase, three small diffraction peaks at 32.55, 42.92, 53.73 degrees appear when the molar ratios of $[CO_3^{2-}]/[Ca^{2+}]$ increased from 3.33 to 6.11. The above 2 theta values were shifted about 0.05 ~ 0.1 degrees to lower 2 theta values, in comparison to the diffraction peaks 32.6, 43.0, 53.7 degrees for $(10\bar{1}4)$, $(11\bar{2}3)$, and $(11\bar{2}6)$ of magnesite, respectively (JCPDS 080479). It is deduced that the above mentioned diffraction peaks in Figure 2 are attributed to the presence of a small amount of Ca^{2+} ion occluded in magnesite. The lattice spacings of Ca-magnesite increase slightly when Mg ion is replaced in magnesite by Ca^{2+} ion with slightly larger atomic size. The Mg contents in the Ca-

magnesite was also calculated by using the $(10\bar{1}4)$ peak shift according to formula (1). With the appearance of Ca-magnesite, the $(10\bar{1}4)$ for Mg-calcite does not shift along with the increase of $[CO_3^{2-}]/[Ca^{2+}]$ ratios in the range of 3.33 - 6.11 (Figure 2b). Besides Mg calcite and Ca-magnesite, a small diffraction peak (001) of brucite ($Mg(OH)_2$) (JCPDS 7-239) appears when the molar ratios of $[CO_3^{2-}]/[Ca^{2+}]$ were in between 5.00 and 6.11. The product includes the primary phase of Mg-calcite and a small amount of Ca-magnesite, brucite, and aragonite at $[CO_3^{2-}]/[Ca^{2+}]$ ratio of 5.00, which is the only case for the appearance of aragonite in this system (Figure 2a), even though aragonite appears very often together with Mg-bearing calcites while the Mg^{2+} was present in the reaction solutions. [22, 25]

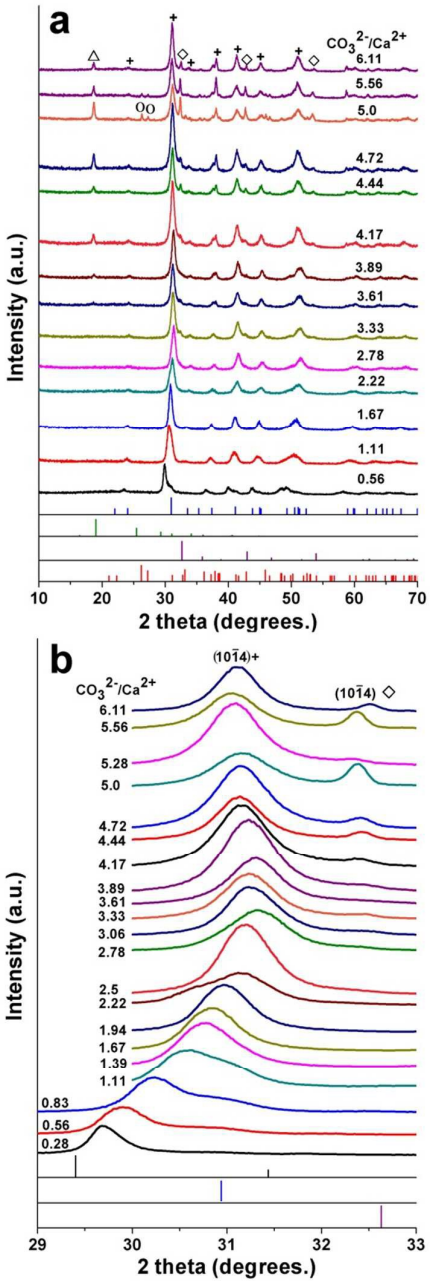

Figure 2. XRD patterns for the calcium carbonate products prepared from mother solutions with varying $[CO_3^{2-}]/[Ca^{2+}]$ ratios at $[Mg^{2+}]/[Ca^{2+}]$ of 2. Meaning of symbols (+: Mg-calcite, ◇: Ca-magnesite, △: brucite, ○: aragonite). Reference patterns: dolomite, Blue, JCPDS 75-1759; magnesite, purple, JCPDS 88-1802; brucite, green, JCPDS 74-2220 and aragonite, red, JCPDS 41-1475.

SEM analysis

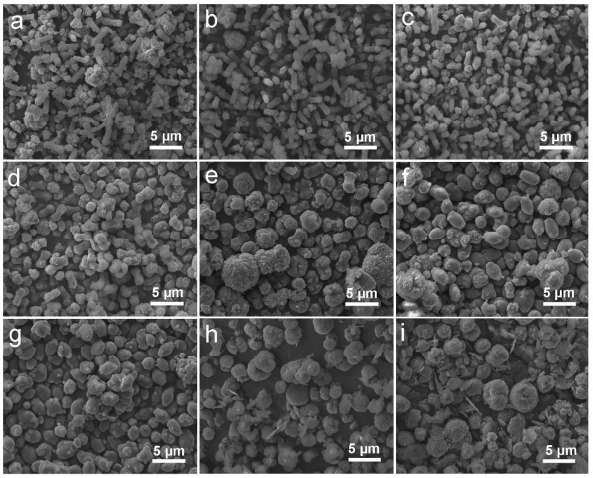

Figure 3 SEM images of the calcium carbonate products prepared from mother solutions with varying $[CO_3^{2-}]/[Ca^{2+}]$ ratios at $[Mg^{2+}]/[Ca^{2+}]$ of 2. The $[CO_3^{2-}]/[Ca^{2+}]$ in the SEM images were (a) 0.28, (b) 1.11, (c) 1.39, (d) 1.67, (e) 2.22, (f) 2.5, (g) 3.33 (h) 3.89, (I) 4.72. The scale bars in images are 5 μm.

SEM characterizations on the samples indicate that the high Mg calcites are short rod-like aggregates of nanoparticles when the molar ratios of $[CO_3^{2-}]/[Ca^{2+}]$ were less than 1.39 (figure 3, a-d). Further increasing the $[CO_3^{2-}]/[Ca^{2+}]$ ratio to 2.5, the morphology of the samples transforms to spindle-like aggregates composed of nanoparticles (figure 3 e, f) , which is similar to the high Mg calcites obtained in the literature.[37] All of the above mentioned products are high Mg calcites in pure phase according to their XRD patterns (Figure 2), even though their morphologies vary with the change of the $[CO_3^{2-}]/[Ca^{2+}]$ ratios (Figure 3 a-f). The spindle shaped aggregates were transformed to spherical aggregates mixed together with a small amount of nanoplates when the molar ratios of $[CO_3^{2-}]/[Ca^{2+}]$ were further increased from 3.33 to 4.72 (figure g-i).

The chemical components for the different carbonate samples were characterized by using Energy-dispersive X-ray spectroscopy (EDS). Two examples were given herein (Figure S1). The short rod-like aggregates obtained at $[CO_3^{2-}]/[Ca^{2+}]$ ratio of 1.39 are composed of elements such as Ca, Mg, C and O according to the EDS analysis (Figure S1 a). EDS analysis indicates that the nanoplates obtained at $[CO_3^{2-}]/[Ca^{2+}]$ ratio of 3.89 were composed

of Mg, C and O (Figure S1 b). Based on the XRD (Figure 2), SEM (Figure 3) and EDS (Figure S 1) characterizations, we propose that the spindle-shaped and spherical shaped aggregates are high Mg calcites while the nanoplates are brucite.

The Mg contents for the Mg calcites in pure phase obtained at $[Mg^{2+}]/[Ca^{2+}]$ ratio of 2 were further characterized in details by using inductively coupled plasma-atomic emission spectrometer (ICP-AES). The Mg contents in the pure phase of Mg-calcites were calculated to be as high as 58 mol% according to the XRD, ICP and EDS characterizations (Figure S2). The Mg contents in the Mg-calcites characterized via ICP were generally higher than the values obtained via XRD and EDS. It is known that the Mg mol% calculated from ICP-AES is the average value of the samples which includes amorphous phase, ACMC, and crystallized Mg-containing calcites while the XRD results only calculated the Mg percentage in the crystallized Mg-calcites. Thus we propose that the Mg content in the ACMC phase is higher than that in Mg-calcite crystals in the products.

FTIR analysis on the high Mg calcites in pure phase

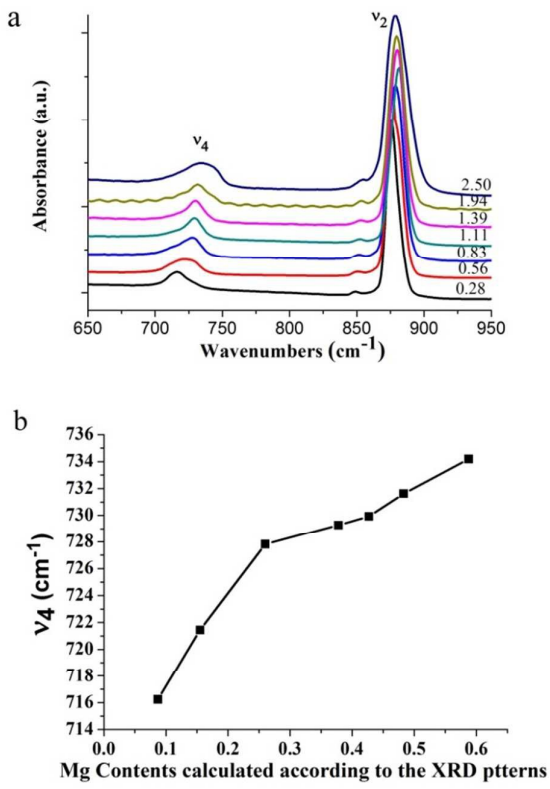

Figure 4. FTIR patterns of Mg-calcites in pure phase obtained at relatively low molar ratios of $[CO_3^{2-}]/[Ca^{2+}]$ while the $[Mg^{2+}]/[Ca^{2+}]$ ratio was 2. (a) FTIR patterns, The molar ratios of $[CO_3^{2-}]/[Ca^{2+}]$ were shown in the spectra. (b) the relationship of v_4 wavenumbers and the Mg contents calculated according to the XRD patterns.

The high Mg calcites in pure phase obtained at $[Mg^{2+}]/[Ca^{2+}]$ molar ratio of 2 were further characterized by using Fourier transform infrared (FTIR) spectroscopy. The absorption band of out-of-plane bending of carbonate, v_4, shifts from 716 cm^{-1} to 737 cm^{-1} while increasing the molar ratios of $[CO_3^{2-}]/[Ca^{2+}]$ from 0.28 to 2.5 (Figure 4). It was known that the absorption band of v_4 shifts to high wavenumbers with the increase of Mg contents in the Mg-calcites.[40] Thus, the higher $[CO_3^{2-}]/[Ca^{2+}]$ molar ratios, the higher wavenumbers for the v_4 absorption band and the higher Mg contents in Mg calcites, consistent with the XRD results (Figure 2). The intensity ratios of the v_2/v_4 peaks for the obtained Mg calcites in pure phase are higher than 7 (Figure 4), much higher than that ratio of the v_2/v_4 peak (2.7) for the geological calcite.[41, 42] The high intensity ratios of the v_2/v_4 peaks indicate that a certain amount of ACMC exists in the high Mg calcite samples,[20, 43] consistent with the ICP and XRD results.

The influences of hydrothermal temperature and time

The influences of the experimental conditions such as the hydrothermal temperature and time for the synthesis of high Mg calcites were investigated while keeping the molar ratio of $[CO_3^{2-}]/[Ca^{2+}]$ as 1.67 and the molar ratio of $[Mg^{2+}]/[Ca^{2+}]$ as 4. The diffraction peaks for the $(10\bar{1}4)$ of Mg-calcites shift slightly to higher 2 theta and the Mg contents in these samples increase from ~47 mol% to ~48 mol% with the increase of hydrothermal temperature from 100 to 150 °C for 24 hours (Figure S3). The Mg contents and standard deviation data in Figure S3 b were calculated according to at least three samples synthesized under the same reaction conditions. Therefore, the hydrothermal temperature variation from 100 to 150 °C does not have much influence for the Mg contents in the final high Mg calcites.

To understand the influence of reaction time for the Mg contents in the final Mg calcites, the hydrothermal time was varied from 2 to 48 hours while keeping the hydrothermal temperature as 150 °C (Figure S4). The Mg contents of the obtained Mg calcites increase slowly from ~45 mol% to ~48 mol% when the heating time was increased from 2 to 24 hours (Figure S4). Further extending hydrothermal time to 48 hours did not influence the Mg content in the Mg calcites. No phase transformation happened even when the hydrothermal time was extended to 5 days in our system, unlike the phase transformation from magnesium calcite to aragonite in a travertine crust specimen[44]. We propose that hydrothermal process at 150 °C for 24 hours is appropriate for the synthesis of well crystallized high Mg calcites in this work. The hydrothermal process for the synthesis of high Mg calcites was kept at 150°C for 24 hours while changing the molar ratios of $[CO_3^{2-}]/[Ca^{2+}]$ and $[Mg^{2+}]/[Ca^{2+}]$ in this work.

Variation of $[Mg^{2+}]/[Ca^{2+}]$ ratios in the mother solutions

The Mg containing calcite samples were further synthesized by changing the molar ratios of $[Mg^{2+}]/[Ca^{2+}]$ to 4 and 6 while keeping the other experimental conditions similar to the above mentioned

system (figure S5 and S6). The XRD patterns for the final products indicate that the primary phases for the products are Mg-containing calcites and Ca-containing magnesites while increasing the molar ratios of $[CO_3^{2-}]/[Ca^{2+}]$ from 0.28 to 6.11 (Figure S5 and S6). With the increase of $[CO_3^{2-}]/[Ca^{2+}]$ molar ratios from 0.28 to 3.06, the final products obtained at $[Mg^{2+}]/[Ca^{2+}]$ of 4 are in the pure phase of Mg-containing calcites and the Mg contents in the Mg-calcites increased from 24 mol% to 63 mol% according to the 2 theta values of the $(10\bar{1}4)$ peak (figure S5). An obvious shoulder peak can be seen from the $(10\bar{1}4)$ peak when the molar ratios of $[CO_3^{2-}]/[Ca^{2+}]$ were 0.28 and 0.56, which indicates that the d-spacings and the Mg contents in these samples are in a wide range (figure S5). Diffraction peaks $(10\bar{1}4)$, $(11\bar{2}3)$, and $(11\bar{2}6)$ of calcium-bearing magnesites are very sharp and strong, indicating there are well crystallized Ca-magnesite crystals mixed together with high Mg calcites when the molar ratios of $[Mg^{2+}]/[Ca^{2+}]$ are 4 and 6 at relatively high molar ratios of $[CO_3^{2-}]/[Ca^{2+}]$ (Figure S5 and S6). The diffraction peak intensities of Ca-magnesite in the samples obtained at $[Mg^{2+}]/[Ca^{2+}]$ ratios of 4 and 6 are much higher than those samples obtained at $[Mg^{2+}]/[Ca^{2+}]$ ratio of 2 (Figure 2, Figure S5 and S6). Thus the high $[Mg^{2+}/Ca^{2+}]$ ratios in the reaction solutions are beneficial for the formation of Ca-containing magnesite. A small diffraction peak, (001) of brucite (JCPDS 7-239) appears from the XRD patterns when the molar ratios of $[CO_3^{2-}]/[Ca^{2+}]$ were higher than 5.56 at $[Mg^{2+}]/[Ca^{2+}]$ of 4.

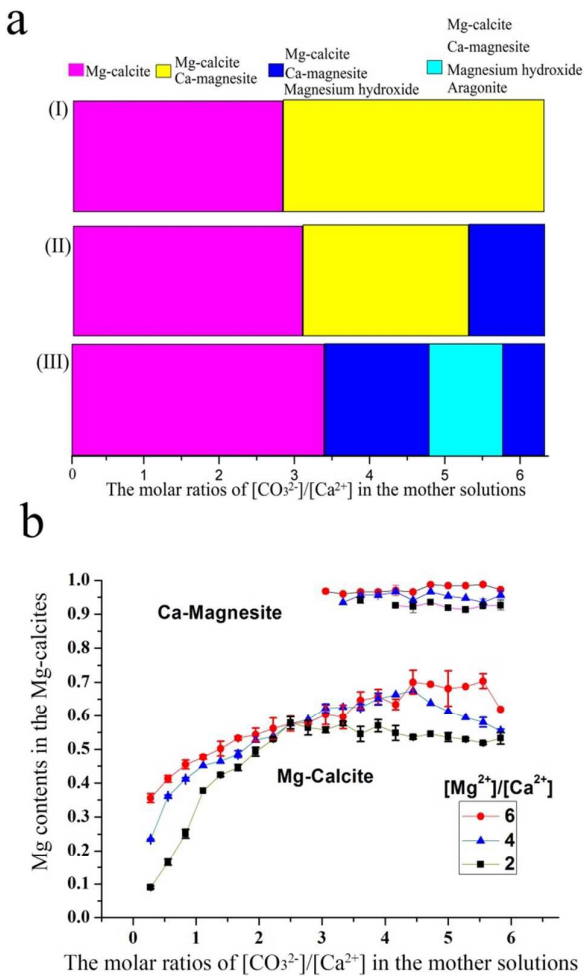

Figure 5. Summary on the polymorphs (a) and the Mg contents (b) in carbonate crystals formed from mother solutions with varying $[CO_3^{2-}]/[Ca^{2+}]$ ratios and $[Mg^{2+}]/[Ca^{2+}]$ ratios.

Figure 5 summarizes the polymorphs of the samples obtained while changing the molar ratios of $[Mg^{2+}]/[Ca^{2+}]$ and the molar ratios of $[CO_3^{2-}]/[Ca^{2+}]$ according to the XRD patterns for these samples (Figure 2, Figure S5 and S6). Hydrothermally unstable phase, high Mg calcites in pure phase can be obtained at relatively low molar ratios of $[CO_3^{2-}]/[Ca^{2+}]$ while increasing the molar ratios of $[Mg^{2+}]/[Ca^{2+}]$ from 2 to 6. It is known that the $[Mg^{2+}]/[Ca^{2+}]$ ratio is important for the Mg contents in the final Mg calcites.[20] In this work, the Mg contents in the Mg calcites in pure phase generally increase with the increase of the molar ratios of $[Mg^{2+}]/[Ca^{2+}]$ under defined $[CO_3^{2-}]/[Ca^{2+}]$ ratios. The effect of the $[Mg^{2+}]/[Ca^{2+}]$ ratios for the Mg contents in Mg-calcites is more obvious at very low molar ratios of $[CO_3^{2-}]/[Ca^{2+}]$. Under a defined $[Mg^{2+}]/[Ca^{2+}]$ ratio, the Mg contents in the high Mg calcites in pure phase increase with the increase of molar ratios of $[CO_3^{2-}]/[Ca^{2+}]$. The concentration of CO_3^{2-} in the mother solution varied from 0.08 mol/L to 0.10 mol/L while the molar ratios of $[CO_3^{2-}]/[Ca^{2+}]$ increased from 0.28 to 6.11, along with the volume variation of the Na_2CO_3 solution added to the metal chloride solution. This is the first time to report the influence of CO_3^{2-} concentration and the molar ratios of $[CO_3^{2-}]/[Ca^{2+}]$ on the synthesis of very high Mg calcites in pure phase in the laboratory.

Mixture of Mg-calcite and Ca-magnesite were formed at relatively high molar ratios of $[CO_3^{2-}]/[Ca^{2+}]$ when the molar ratios of $[Mg^{2+}]/[Ca^{2+}]$ are 4 and 6. Furthermore, the brucite appeared together with Mg-calcite and Ca-magnesite at relatively high molar ratios of $[CO_3^{2-}]/[Ca^{2+}]$, 3.61-6.11 for $[Mg^{2+}]/[Ca^{2+}]$=2, 5.56-6.11 for $[Mg^{2+}]/[Ca^{2+}]$=4. The pH values for the supernatant solutions for the above reaction systems after the hydrothermal process are higher than 9.0 (Table S1). No brucite was formed when the pH values of the supernatant reaction solutions were all below 7.4 at $[Mg^{2+}]/[Ca^{2+}]$ of 6. Representative results for the pH values of the supernatant solutions after the hydrothermal process were shown in Table S1. Based on the above experimental results, it can be concluded that a certain amount of redundant Na_2CO_3 and the alkaline environment were necessary for the formation of brucite in this system.

It is known from the literature that the Ksp values of calcite and magnesite in water are $4.49*10^{-9}$ [45, 46] and $10^{-9.47}$, [47] respectively. The Ksp for ACC is about $4*10^{-6}$.[46] The concentration for free Ca^{2+} and CO_3^{2-} in the solution is about $2*10^{-3}$ mol/L. Herein, we assume the concentrations for the free Ca^{2+}, Mg^{2+} and CO_3^{2-} are $2*10^{-3}$ mol/L at maximum. To make a balance for the carbonate group and the metal ions in the reaction solutions, the molar ratios of $[CO_3^{2-}]/[Ca^{2+}]$ should be 3 and 5 while the molar ratios of $[Mg^{2+}]/[Ca^{2+}]$ are 2 and 4, respectively. In our system, brucite was formed under alkaline environment only when the $[CO_3^{2-}]/[Ca^{2+}]$ ratios are higher than 3 and 5 (3.61 and 5.56) at $[Mg^{2+}]/[Ca^{2+}]$ ratios of 2 and 4, respectively.

Conclusion

We studied the influences of the carbonate concentration and the $[CO_3^{2-}]/[Ca^{2+}]$ molar ratios for the Mg contents in the high Mg calcites in details in this work. High Mg calcites in pure phase with controlled magnesium contents were synthesized for the first time by using ACMC as intermediate precursor through a hydrothermal process in the absence of organic additives. Besides the molar ratios of $[Mg^{2+}]/[Ca^{2+}]$, our study shows that the molar ratio of $[CO_3^{2-}]/[Ca^{2+}]$ in the mother solutions is also a very important factor for the Mg contents occluded in the high Mg-calcites. The Mg contents in the Mg-containing calcites increase from 10 to 63 mol% by increasing the CO_3^{2-} concentration and the molar ratios of $[CO_3^{2-}]/[Ca^{2+}]$ in the mother solutions in this work. The higher molar ratios of $[CO_3^{2-}]/[Ca^{2+}]$ in the mother solutions, the higher Mg contents in Mg calcites in pure phase, at relatively low carbonate concentrations. Further increase of the $[CO_3^{2-}]/[Ca^{2+}]$ ratios in the mother solutions results in the formation of other polymorphs such as Ca-magnesite, brucite, or aragonite. Studies on the formation process of thermodynamically unstable biogenic high-Mg calcites in the laboratories may shed light on the preparation of functional materials with enhanced mechanical properties.

Experimental Section

Materials and methods:

Magnesium chloride hexahydrate ($MgCl_2{\cdot}6H_2O$), calcium chloride dehydrate ($CaCl_2{\cdot}2H_2O$) and sodium carbonate (Na_2CO_3) were bought from Alfa Aesar.

Preparation of intermediate powder precursor:

Typically, a precursor suspension was prepared by quickly mixing Na_2CO_3 solution (2 mol/L) with 9 mL of mixed solution of $MgCl_2$ and $CaCl_2$ (0.1 mol/L) ($[Mg^{2+}]/[Ca^{2+}]$=2; 4; 6) at 4 °C. The volume of Na_2CO_3 solution was defined by the molar ratios of $[CO_3^{2-}]$ and $[Ca^{2+}]$. A cloudy suspension formed immediately, indicating the formation of colloid particles in the solution. For characterization, the freshly prepared suspension was quickly filtered under vacuum and washed with double distilled water and alcohol in sequence. The obtained powder precursor was later used for characterization by XRD, SEM and TEM.

Hydrothermal process for the synthesis of high Mg calcites:

In a typical synthesis, the freshly prepared cloudy suspension was kept at 150 °C for 24 hours in a Teflon autoclave with a capacity of 20 mL, if not mentioned specifically. The supernatant was poured and the product at the bottom was centrifuged and washed with double distilled water for three times and then washed with ethanol for one time. The final products were dried in a drying oven under vacuum at 70 °C for 24 h.

Characterizations

X-ray diffraction (XRD) patterns of the products were determined using a Rigaku Dmax-2000. The XRD patterns for the products were generally recorded with a step size of 4 °/min from10 to 70 °. To get more quantitative data for the 2 theta values of (104) peak of Mg-calcite and Ca-magnesite, diffraction patterns were further recorded in the 2 theta of 29 ~ 33 ° with a step size of 0.2 °/min.

The samples were characterized by using scanning electron microscopy (SEM) images and the Energy-dispersive X-ray spectroscopy (EDS) analysis on FEI Nano 430 at an accelerating voltage of 8.0 kV and 14.0 kV, respectively. Transmission electron microscopy (TEM) images and electron diffraction were recorded on a JEOL JEM-200CX at 160 kV.

The final products were further characterized in detail with Fourier transform infrared spectrometer (FTIR, VECTOR22) and inductively coupled plasma-atomic emission spectrometer (ICP-AES, PROFILE SPEC, Leeman) analysis.

The pH values of the reaction suspensions after the hydrothermal process were recorded by a Mettler pH meter (PE20).

Acknowledgements

Financial supports from the National Natural Science Foundation of China (Grant Nos. 51272298, 21073005, and 51121091) are gratefully acknowledged.

Notes and references

1. K. E. Chave, K. S. Deffeyes, P. K. Weil, R. M. Garrels and M. E. Thompson, *Science*, 1962, **157**, 33.
2. S. Raz, S. Weiner and L. Addadi, *Adv. Mater.*, 2000, **12**, 38.
3. X. Long, Y. R. Ma and L. M. Qi, *J. Struct. Biol.*, 2014, **185**, 1.
4. J. R. Goldsmith, D. L. Graf and H. C. Heard, *Am. Miner.*, 1961, **46**, 453.
5. S. E. Kaczmarek and D. F. Sibley, *Sedimentary Geology*, 2011, **240**, 30.
6. G. Montes-Hernandez, N. Findling, F. Renard and A. L. Auzende, *Cryst. Growth Des.*, 2014, **14**, 671.
7. S. M. Stanley, J. B. Ries and L. A. Hardie, *P. Natl. Acad. Sci. U.S.A.*, 2002, **99**, 15323.
8. K. E. Chave, *J. Geol.*, 1954, **62**, 266.
9. J. H. Schroeder, E. J. Dwornik and J. J. Papike, *Geol. Soc. Am. Bull.*, 1969, **80**, 1613.
10. Y. R. Ma, B. Aichmayer, O. Paris, P. Fratzl, A. Meibom, R. A. Metzler, Y. Politi, L. Addadi, P. Gilbert and S. Weiner, *Proc. Natl. Acad. Sci. U. S. A.*, 2009, **106**, 6048.
11. S. Gayathri, R. Lakshminarayanan, J. C. Weaver, D. E. Morse, R. M. Kini and S. Valiyaveettil, *Chem. Eur. J.*, 2007, **13**, 3262.
12. Y. Ma, S. Weiner and L. Addadi, *Adv. Funct. Mater.*, 2007, **17**, 2693.
13. C. E. Killian, R. A. Metzler, Y. U. T. Gong, I. C. Olson, J. Aizenberg, Y. Politi, F. H. Wilt, A. Scholl, A. Young, A. Doran, M. Kunz, N. Tamura, S. N. Coppersmith and P. U. P. A. Gilbert, *J. Am. Chem. Soc.*, 2009, **131**, 18404.
14. X. Long, M. J. Nasse, Y. R. Ma and L. M. Qi, *Phys. Chem. Chem. Phys.*, 2012, **14**, 2255.
15. J. Seto, Y. R. Ma, S. A. Davis, F. Meldrum, A. Gourrier, Y. Y. Kim, U. Schilde, M. Sztucki, M. Burghammer, S. Maltsev, C. Jager and H. Colfen, *Proc. Natl. Acad. Sci. U. S. A.*, 2012, **109**, 3699.
16. L. Addadi, S. Raz and S. Weiner, *Adv. Mater.*, 2003, **15**, 959.

17. J. H. Tao, D. M. Zhou, Z. S. Zhang, X. R. Xu and R. K. Tang, *Proc. Natl. Acad. Sci. U. S. A.*, 2009, **106**, 22096.
18. Y. Ma, S. R. Cohen, L. Addadi and S. Weiner, *Adv. Mater.*, 2008, **20**, 1555.
19. M. E. Kunitake, S. P. Baker and L. A. Estroff, *MRS Commun.*, 2012, **2**, 113.
20. X. Long, Y. Ma and L. Qi, *Crystal Growth Des.*, 2011, **11**, 2866.
21. J. Jiang, M.-R. Gao, Y.-H. Qiu, G.-S. Wang, L. Liu, G.-B. Cai and S.-H. Yu, *CrystEngComm*, 2011, **13**, 952.
22. G. Falini, M. Gazzano and A. Ripamonti, *Chem. Commun.*, 1996, 1037.
23. G. Falini, S. Fermani, M. Gazzano and A. Ripamonti, *J. Mater. Chem.*, 1998, **8**, 1061.
24. Y.-Y. Liu, J. Jiang, M.-R. Gao, B. Yu, L.-B. Mao and S.-H. Yu, *Crystal Growth & Design*, 2012, **13**, 59.
25. J. J. Lenders, A. Dey, P. H. Bomans, J. Spielmann, M. M. Hendrix, G. de With, F. C. Meldrum, S. Harder and N. A. Sommerdijk, *J. Am. Chem. Soc.*, 2012, **134**, 1367.
26. I. Sethmann, J. Wang, U. Becker and A. Putnis, *Cryst. Growth Des.*, 2010, **10**, 4319.
27. N. Wada, K. Yamashita and T. Umegaki, *J. colloid interface sci.*, 1999, **212**, 357.
28. Y.-J. Han and J. Aizenberg, *J. Am. Chem. Soc.*, 2003, **125**, 4032.
29. X. Cheng, P. L. Varona, M. J. Olszta and L. B. Gower, *J. cryst. growth*, 2007, **307**, 395.
30. D. Wang, A. F. Wallace, J. J. De Yoreo and P. M. Dove, *Proc. Natl. Acad. Sci. U. S. A.*, 2009, **106**, 21511.
31. J. Xiao and S. Yang, *CrystEngComm*, 2011, **13**, 2472.
32. F. Zhang, H. Xu, H. Konishi, E. S. Shelobolina and E. E. Roden, *Am. Miner.*, 2012, **97**, 556.
33. N. Han, C. R. Blue, J. De Yoreo and P. M. Dove, *Proceedings of the Fourteenth International Symposium on Water-Rock Interaction, Wri 14*, 2013, **7**, 223.
34. A. Stephenson, J. DeYoreo, L. Wu, K. Wu, J. Hoyer and P. Dove, *Science*, 2008, **322**, 724.
35. M. E. Maguire and J. A. Cowan, *Biometals*, 2002, **15**, 203.
36. M. Pavlov, P. E. Siegbahn and M. Sandström, *J. Phys. Chem. A*, 1998, **102**, 219.
37. J. Xu, C. Yan, F. Zhang, H. Konishi, H. Xu and H. H. Teng, *Proc. Natl. Acad. Sci. U. S. A.*, 2013, **110**, 17750.
38. J. C. Orr, V. J. Fabry, O. Aumont, L. Bopp, S. C. Doney, R. A. Feely, A. Gnanadesikan, N. Gruber, A. Ishida, F. Joos, R. M. Key, K. Lindsay, E. Maier-Reimer, R. Matear, P. Monfray, A. Mouchet, R. G. Najjar, G. K. Plattner, K. B. Rodgers, C. L. Sabine, J. L. Sarmiento, R. Schlitzer, R. D. Slater, I. J. Totterdell, M. F. Weirig, Y. Yamanaka and A. Yool, *Nature*, 2005, **437**, 681.
39. A. Niedermayr, S. J. Kohler and M. Dietzel, *Chem. Geol.*, 2013, **340**, 105.
40. Y. Dauphin, *Appl. spectrosc.*, 1999, **53**, 184.
41. E. Beniash, J. Aizenberg, L. Addadi and S. Weiner, *Proceedings of the Royal Society B-Biological Sciences*, 1997, **264**, 461.
42. Y. Politi, T. Arad, E. Klein, S. Weiner and L. Addadi, *Science*, 2004, **306**, 1161.
43. Y. Politi, Y. Levi-Kalisman, S. Raz, F. Wilt, L. Addadi, S. Weiner and I. Sagi, *Adv. Funct. Mater.*, 2006, **16**, 1289.
44. H. F. Greer, W. Z. Zhou and L. Guo, *Mineral. Petrol.*, 2015, **109**, 453.
45. F. Lippmann, *Sedimentary Carbonate Minerals*, Berlin, 1973.
46. D. Gebauer, A. Volkel and H. Colfen, *Science*, 2008, **322**, 1819.
47. P. Benezeth, G. D. Saldi, J. L. Dandurand and J. Schott, *Chem. Geol.*, 2011, **286**, 21.